Rapp. P.-v. Réun. Cons. int. Explor. Mer, 170: 223–231. Février 1977.

THE EFFECTS OF INTERNAL WAVES ON FISH SCHOOL MAPPING WITH SONAR IN THE CALIFORNIA CURRENT AREA

P. E. Smith

U.S. Department of Commerce, National Oceanic and Atmospheric Administration,
National Marine Fisheries Service, Southwest Fisheries Center, La Jolla, California 92037, USA

Sonar mapping of schools of fish in surface waters where echo-sounders are ineffective is influenced by changes in the effective range of detection caused by changes in the sound velocity profile as well as by vertical migrations and changes in packing density within the schools.

Analysis has been made of 38 sound velocity profiles over a short period in one region and their variation compared with that in a mass of data for the California area; the short-term variation was of comparable magnitude to that over a 20 year period, with effective detection range varying five-fold. As analysis of the sound velocity profiles at each school mapping station is impractical, a statistical approach is made to determine an 'average' effective detection range. This utilizes historical data, partitions areas and seasons according to intensity of variation in the sound velocity data, allocates sound velocity profiling so as to reduce the standard error of the mean sound velocity gradients in upper waters to a uniform value for all areas and seasons and then, for these profiles, creates a probability diagram for corrections to the number of targets detected at various ranges and depths. An example of the application of the method is given.

INTRODUCTION

Fish school mapping with sonar is a technique developed (Smith, 1970) to study the schools of the northern anchovy, *Engraulis mordax*, which are abundant in the California Current region off the west coast of North America. Sonar mapping provides estimates of the horizontal dimensions of fish schools and an estimate of the number of fish schools and their cross-sectional area per unit area surveyed. This technique was developed because fish schools are frequently found in the upper mixed layer of the ocean where echo-sounders are relatively ineffectual at counting or measuring them. The following difficulties have been noted for echo-sounder surveys for fish schools: (1) These schools may be shallower than the echo-sounder installation or within the zone below the echo-sounder where the outgoing pulsed emission precludes target reception. (2) Biases in estimating the depth, thickness, and compaction of the school may result from the reaction of fish to the approaching ship. (3) The transect of the ship over the school only infrequently coincides with the major or minor axes of the school, thus leading to biased estimates of horizontal school dimensions. (4) Multiple echo returns from near-surface schools may lead to biased estimates of school thickness. The major biases of the sonar mapping technique are changes in effective range of detection caused by changes in packing density within the schools, vertical migration of the schools, and regional, seasonal and short-term changes in the sound velocity profile. However, the range of detection is frequently tens to hundreds of times the width of the echo-sounder beam, and a much larger sample of fish schools is obtained per unit ship time.

Prior to an error evaluation cruise in 1968 (Smith, 1970), it was planned that repetitive temperature profiles would be taken to enable description and analysis to be made of internal waves and their attendant ray tracing profiles in the tidal period part of the internal wave spectrum. The expected tidal period was not as important as internal waves which had shorter periods and higher amplitudes. Relatively coherent time changes were observed at 5-minute intervals. Temporal changes of this order implied spatial changes in the temperature profile which could not reasonably be monitored from a moving ship. Thus, the expense of measuring and analyzing these changes for all fish school mapping surveys appeared prohibitive. An effective range estimate is essential to quantitative surveys, and a statistical approach to the definition of the "average" effective range was sought. The 38 profiles taken for the coherent analysis of the tidal period internal waves were then reanalyzed as though they were independent samples of the effective range in this area. The variability in the temperature and sound velocity gradients in this 3-day example was then

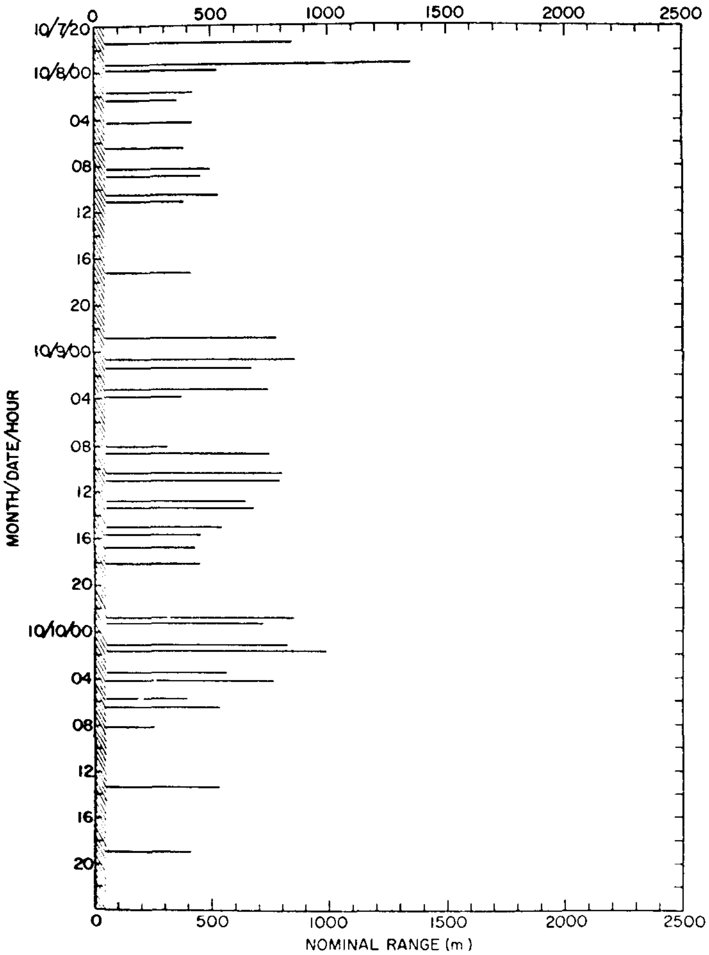

Figure 205. Chronological order of ray trace model derived detection range of −30 dB sonar target at 20 m depth off Santa Catalina Island, California in October 1968.

compared with the climatic variability in these properties as revealed by long-term records of these properties in this and other regions and seasons.

It is the purpose of this paper to examine the importance and tractability of the internal wave problem with regard to applying unbiased estimates of transmission loss to the description of the probability of target detection by range and depth and the measurement of target strength of those targets received. The analysis and description of the 38 test-temperature profiles will be reported, the variability in thermal and sound velocity profiles will be compared with statistical summaries of hydrographic and bathythermographic measurements taken in California Current area, and a procedure for the allocation of sound velocity estimation effort for an unbiased description of effective sonar range by region and season will be derived.

SOURCES OF DATA

All climatic data were obtained from the archives of the National Oceanographic Data Center of the Environmental Data Service of the National Oceanic and Atmospheric Administration of the United States Department of Commerce. The temperatures, salinities and sound velocities were obtained from approximately 11 000 hydrographic stations at each of 12 depths above 300 m. These include all the stations archived for the area under consideration since 1939. In addition the temperatures were obtained from the 33 183 bathythermograph (BT) profiles taken in this area since 1939 in which temperatures were recorded every 5 m in the upper 45 m. This latter file apparently contains 2·6 % of all BT's ever taken (Couper and LaFond, 1970) and 13·8 % of those taken in the Pacific. A crude attempt to remove the bias of sound velocity calculations from temperature profiles was to apply average salinities by depth, month and year to each of the temperature profiles. Another analysis of the thermal profiles used a constant salinity of 34 ‰.

The rapid sequence expendable bathythermograph (XBT) data were taken by Sippican* equipment from the RV "David Starr Jordan" while underway at ca. 11 knots. The data were digitized manually by 5 m inter-

* This does not constitute endorsement of this commercial product by the U.S. Government.

Table 44. Sound velocity profiles (m sec^{-1}) evaluated for range of detection of − 30 dB sonar target at 20 m depth

Short range

Depth m	Time 0812 Range 256 m	Time 0806 Range 311 m	Time 0222 Range 357 m	Time 0351 Range 375 m	Time 0630 Range 384 m	Time 1106 Range 384 m	Time 0543 Range 393 m	Time 1712 Range 411 m	Time 1856 Range 411 m	Time 0143 Range 421 m	Time 0419 Range 421 m	Time 1650 Range 430 m	Time 1809 Range 448 m
0	1517·0	1516·2	1517·0	1519·3	1517·0	1517·9	1516·7	1517·9	1516·7	1517·9	1517·9	1518·7	1518·7
5	1515·1	1515·1	1516·3	1517·4	1516·5	1516·3	1516·3	1516·5	1516·3	1516·5	1516·8	1517·4	1517·7
10	1505·8	1509·0	1511·2	1516·0	1510·5	1515·2	1510·5	1516·0	1512·1	1516·0	1516·0	1516·6	1516·6
15	1502·6	1501·6	1508·1	1513·4	1505·9	1510·6	1507·4	1507·4	1507·1	1507·4	1507·4	1513·1	1513·7
20	1501·1	1500·1	1504·6	1509·1	1503·7	1505·9	1503·3	1504·0	1504·0	1505·6	1501·7	1505·9	1509·1
25	1500·5	1499·8	1502·8	1507·6	1499·5	1502·8	1501·1	1501·1	1502·8	1501·8	1498·8	1503·7	1504·4
30	1497·9	1498·2	1501·2	1503·5	1497·9	1500·2	1500·2	1499·2	1500·9	1501·5	1498·9	1501·5	1502·2
35	1497·3	1497·6	1497·3	1501·3	1497·3	1498·0	1498·0	1497·6	1498·3	1499·6	1498·6	1500·3	1499·3
40	1497·4	1495·7	1496·4	1499·7	1495·7	1497·7	1497·7	1496·0	1497·7	1499·4	1497·4	1499·0	1497·7
45	1495·4	1495·1	1495·1	1498·1	1495·5	1497·1	1495·1	1495·1	1496·1	1497·5	1495·4	1497·1	1495·8
50	1494·8	1494·1	1493·4	1495·9	1495·2	1495·5	1493·1	1494·5	1494·5	1495·2	1495·2	1495·9	1494·5
70	1491·3	1491·3	1491·0	1491·7	1491·7	1492·0	1491·3	1491·3	1491·0	1492·4	1491·7	1492·7	1490·6
90	1490·0	1490·0	1490·3	1490·9	1490·0	1490·9	1490·0	1490·3	1489·7	1490·3	1489·3	1490·0	1489·7
110	1489·7	1490·0	1490·0	1490·6	1489·7	1490·6	1490·0	1489·7	1489·0	1490·0	1489·3	1489·7	1489·7
130	1490·0	1489·6	1490·0	1490·3	1489·6	1490·3	1489·0	1489·0	1488·7	1490·0	1489·0	1489·6	1489·6
150	1490·0	1489·3	1490·0	1490·3	1489·6	1489·6	1489·0	1489·0	1489·3	1489·6	1488·7	1490·0	1489·3

Medium range

Depth m	Time 0850 Range 457 m	Time 1544 Range 457 m	Time 0817 Range 494 m	Time 2349 Range 521 m	Time 1033 Range 530 m	Time 1325 Range 530 m	Time 0627 Range 539 m	Time 1503 Range 549 m	Time 0332 Range 558 m	Time 1246 Range 649 m	Time 0121 Range 677 m	Time 1321 Range 686 m	Time 2318 Range 722 m
0	1516·5	1518·5	1516·7	1516·5	1518·7	1517·9	1516·2	1517·3	1516·7	1517·9	1517·0	1518·2	1517·0
5	1516·0	1517·4	1516·5	1516·0	1517·1	1516·5	1516·3	1516·3	1516·5	1516·5	1516·5	1517·1	1516·8
10	1514·0	1516·6	1510·5	1514·9	1516·9	1516·6	1509·0	1516·0	1513·3	1516·3	1516·3	1516·9	1516·3
15	1505·9	1512·8	1504·2	1510·6	1516·4	1512·2	1505·9	1513·7	1510·0	1516·1	1513·7	1516·7	1510·9
20	1504·0	1507·2	1499·1	1508·2	1512·3	1508·5	1503·0	1510·7	1508·2	1515·9	1510·4	1516·2	1505·9
25	1500·1	1505·0	1498·5	1503·7	1507·6	1502·8	1501·8	1504·4	1506·0	1510·8	1503·7	1506·0	1502·8
30	1500·2	1501·9	1496·9	1501·9	1503·8	1500·6	1499·2	1500·6	1501·5	1504·5	1501·5	1502·2	1499·6
35	1497·3	1499·3	1495·3	1498·6	1500·3	1499·3	1497·0	1498·3	1498·6	1501·3	1499·0	1499·3	1498·0
40	1496·7	1497·7	1495·0	1497·7	1499·0	1499·0	1496·0	1497·7	1497·0	1499·7	1497·0	1498·1	1497·0
45	1495·1	1497·1	1494·0	1496·8	1497·1	1497·5	1494·7	1495·8	1495·4	1497·8	1495·4	1497·1	1496·5
50	1494·8	1496·2	1493·4	1495·5	1495·9	1496·9	1493·8	1495·2	1493·8	1496·5	1494·5	1495·5	1495·2
70	1491·3	1492·4	1491·7	1492·0	1493·8	1492·0	1490·6	1492·0	1491·0	1492·4	1490·6	1490·6	1492·9
90	1489·7	1490·6	1490·3	1490·6	1490·9	1490·3	1489·7	1490·6	1490·0	1490·3	1490·3	1490·0	1490·0
110	1489·3	1490·0	1490·0	1490·3	1490·3	1489·7	1489·3	1489·7	1489·3	1489·7	1490·3	1489·7	1489·7
130	1488·7	1490·0	1489·6	1490·0	1490·0	1489·6	1489·6	1490·0	1489·0	1489·6	1490·0	1489·6	1489·3
150	1488·7	1490·3	1489·0	1489·6	1490·0	1489·6	1490·0	1489·3	1489·3	1489·6	1490·3	1490·0	1489·6

(To be continued.)

Table 44 (continued).

Long range

Depth m	Time 0312 Range 741 m	Time 0839 Range 750 m	Time 0409 Range 759 m	Time 2250 Range 777 m	Time 1057 Range 796 m	Time 1025 Range 805 m	Time 0109 Range 823 m	Time 2129 Range 850 m	Time 2248 Range 850 m	Time 0041 Range 860 m	Time 0144 Range 988 m	Time 2315 Range 1344 m
0	1517·0	1517·0	1516·2	1517·3	1516·5	1516·5	1516·5	1516·7	1517·0	1517·9	1517·0	1516·5
5	1516·5	1517·1	1516·3	1517·1	1516·3	1516·3	1516·3	1516·3	1516·3	1517·4	1517·1	1516·3
10	1516·3	1516·3	1515·2	1516·6	1516·0	1516·3	1516·0	1516·3	1516·3	1517·5	1517·2	1516·3
15	1515·6	1511·2	1507·4	1514·3	1510·6	1515·0	1515·8	1516·4	1516·1	1516·7	1517·3	1516·4
20	1510·7	1506·9	1505·6	1512·3	1504·3	1504·0	1509·1	1510·7	1512·0	1515·0	1516·8	1516·5
25	1503·7	1504·1	1501·1	1504·4	1501·1	1502·8	1503·4	1502·8	1508·6	1506·0	1514·5	1510·8
30	1501·2	1501·2	1498·2	1500·9	1499·9	1501·2	1499·9	1501·2	1502·9	1500·6	1507·7	1506·4
35	1500·3	1498·6	1496·3	1499·6	1498·6	1499·0	1498·6	1498·0	1500·3	1499·6	1502·0	1501·3
40	1498·7	1498·4	1495·7	1498·4	1497·4	1498·1	1497·7	1497·0	1499·4	1498·1	1499·4	1498·7
45	1496·5	1497·1	1494·7	1497·5	1496·8	1496·1	1495·4	1495·4	1499·1	1496·5	1497·5	1496·5
50	1495·5	1496·5	1493·8	1495·2	1495·5	1495·9	1495·2	1495·2	1495·2	1495·2	1496·2	1494·5
70	1492·4	1494·8	1490·6	1491·7	1492·7	1494·1	1492·0	1491·3	1491·7	1492·4	1492·0	1491·3
90	1490·3	1492·7	1489·7	1490·6	1490·9	1492·3	1490·0	1491·6	1490·0	1491·6	1490·6	1490·3
110	1490·0	1492·3	1489·7	1490·6	1490·3	1492·0	1490·0	1493·4	1490·0	1491·2	1490·3	1490·0
130	1489·6	1492·3	1489·6	1490·6	1490·0	1491·9	1489·6	1494·7	1489·0	1491·3	1490·3	1489·6
150	1489·6	1492·6	1490·0	1490·3	1490·3	1491·6	1489·6	1494·0	1489·6	1491·3	1490·6	1490·0

vals from the surface to 50 m and by 20 m intervals from 50 to 450 m. Characteristic salinities were taken from a T-S diagram for this area and season.

METHODS OF ANALYSIS

The ray tracing program was operated by the Ocean Operations Project of the U.S. Navy Fleet Numerical Weather Central, Monterey, California. Parameters of the program included a source depth of 3·65 m, target depths of 4, 10, 20, and 50 m, source frequencies of 11, 29·8, and 75 kHz, arbitrary surface and bottom characterizations, and stepping angles of 0·2° from 0·02° to 14·76° down and 0·05° from 15·00° to 30·00° down, with a transducer which is 10° between the 3 dB down points and declined downwards 4° from the surface. Estimates of transmission loss to the four target depths were reported in 10 yard intervals to a point that exceeded the combined threshold specified by minimum target strength (−30 dB), receiver sensitivity, source level, and attenuation. Transmission loss variations were evaluated at 29·8 kHz, for targets at 20 m depth, at ranges of 250 and 300 m.

Table 45. Mean gradients ($m_x \sec^{-1} m_z^{-1}$) for the sound velocity profiles in the upper 30 m

Depth (m)	Detection range: Short	Medium	Long
0	− 0·2	− 0·1	− 0·0
5	− 0·7	− 0·3	− 0·1
10	− 1·0	− 0·6	− 0·4
15	− 0·7	− 0·6	− 0·8
20	− 0·5	− 0·9	− 1·0
25	− 0·4	− 0·6	− 0·7
30	− 0·4	− 0·5	− 0·5

RESULTS

The data were examined to determine the effects of transmission loss variations on target detection. The maximum range of detection varied from 256 to 1344 m in the 38 ray trace analyses. There were modes at detection ranges of 400 and 800 m. These detection ranges are illustrated in chronological order in Figure 205. The detection range at a target depth of 20 m has been used for an index of effective range. In Table 44 the thermal profiles are listed in increasing order of the effective range and are arbitrarily divided into short range (< 450 m), medium range (450–750 m), and long range (> 750 m). The variation in detection range is apparently caused by changes taking place in the thermal profile in the upper 30 m. For all three range categories the mean slope for the sound velocity profile is 0·5 metres per second per metre depth ($m_x \sec^{-1} m_z^{-1}$) between the surface and 35 m. It is apparent from Table 45 that the differences are caused by the distribution and intensity of the gradients in the upper layer.

To see whether this series of thermal profile samples taken in October of 1968 is representative of the kinds

Table 46. Statistical summary of sound velocity and sound velocity gradient profiles and comparison between October 1968 and long-term regional profiles in October; sound velocity in m/s, and sound gradient in m/s/m depth

Depth m	Short term: Sound velocity $\bar{X}$	Short term: Sound velocity S	Short term: Sound gradient $\bar{X}$	Short term: Sound gradient S	s.e.$\bar{X}$	Long term: Sound velocity $\bar{X}$	Long term: Sound velocity S	Long term: Sound gradient $\bar{X}$	Long term: Sound gradient S
0	1517·3	0·82	−0·1426	0·117	0·019	1515·7	4·48	−0·1170	0·201
5	1516·6	0·56	−0·3558	0·500	0·081				
10	1514·8	2·83	−0·7042	0·544	0·088	1514·6	5·17	−0·4483	0·352
15	1511·3	4·42	−0·7158	0·446	0·072				
20	1507·9	5·02	−0·7816	0·488	0·079	1510·0	5·94	−0·4993	0·277
25	1503·8	3·44	−0·5484	0·324	0·053				
30	1501·0	2·20	−0·4458	0·235	0·038	1505·0	6·20	−0·3487	0·148
35	1498·8	1·45	−0·2221	0·128	0·021				
40	1497·7	1·22	−0·2858	0·123	0·020				
45	1496·3	1·13	−0·2347	0·150	0·024				
50	1495·1	0·90	−0·1629	0·038	0·006	1497·9	4·78	−0·1633	0·095
70	1491·8	0·94	−0·0700	0·032	0·005				
75						1493·7	3·42	−0·0922	0·069
90	1490·4	0·71	−0·0146	0·022	0·004				
100						1491·4	2·61	−0·0439	0·041
110	1490·1	0·86	−0·0091	0·019	0·003				
125						1490·3	2·29	−0·0298	0·029
130	1490·0	1·09	0·0004	0·018	0·003				
150	1490·0	1·02	0·0041	0·018	0·003	1489·5	2·22	−0·0173	0·019

of gradients to be expected in this area at this season, the average profile for the 38 samples in 1968 is compared with the long-term average for all profiles taken in hydrographic casts in this area in October since 1939 (Table 46). Both the sound velocities and the sound velocity gradients are within the expected range.

In a consideration of the effects of transmission loss variations on target strength determination, the data

Table 47. Variations in transmission loss

Time	20 m range (m)	250 m Transmis. loss A (dB km⁻¹)	300 m Transmis. loss B (dB km⁻¹)	A to B Transmis. loss C (dB km⁻¹)	Time	20 m range (m)	250 m Transmis. loss A (dB km⁻¹)	300 m Transmis. loss B (dB km⁻¹)	A to B Transmis. loss C (dB km⁻¹)
		Short					Medium		
0812	256	204	–	–	0627	539	208	189	100
0806	311	206	181	65	1503	549	196	169	46
0222	357	201	178	75	0332	558	197	173	65
0351	375	196	168	43	1246	649	193	163	31
0630	384	206	182	75	0121	677	197	171	55
1106	384	197	170	48	1321	686	195	166	36
0543	393	204	182	83	2318	722	201	176	60
1712	411	202	175	52	0312	741	197	171	54
1856	411	201	179	79					
0143	421	201	173	45			Long		
0419	421	204	176	53	0839	750	201	175	60
1650	430	200	172	46	0409	759	201	176	65
1809	448	197	171	49	2250	777	196	169	48
					1057	796	204	177	57
		Medium			1025	805	204	177	53
0850	457	201	176	65	0109	823	200	173	56
1544	457	199	172	54	2129	850	199	172	50
0817	494	210	188	86	2248	850	197	171	56
2349	521	198	170	48	0041	860	195	167	39
1033	530	195	169	50	0144	988	194	166	39
1325	530	199	172	50	2315	1344	193	163	31

Table 48. Bathythermograph-derived maximum standard deviation of sound velocity gradient (m_x sec^{-1} m_z^{-1}) in the upper 30 m by region and month

Month/Region	CCI	CCO	SCI	SCO	SCS	BCI	BCO	BCS	SBI	SBO
Jan	0·08	0·10	0·16	0·14	0·08	0·15	0·09	0·06	0·21	0·06
Feb	0·08	0·09	0·13	0·10	0·06	0·14	0·14	0·07	0·14	0·07
Mar	0·15	0·08	0·18	0·12	0·07	0·15	0·08	0·10	0·18	0·12
Apr	0·31	0·14	0·27	0·16	0·08	0·23	0·09	0·10	0·24	0·10
May	0·21	0·17	0·35	0·20	0·19	0·28	0·18	0·18	0·28	0·14
Jun	0·25	0·26	0·48	0·29	0·19	0·35	0·17	0·13	0·31	0·32
Jul	0·46	0·31	0·56	0·36	0·26	0·43	0·26	0·16	0·67	0·44
Aug	0·30	0·46	0·58	0·42	0·29	0·44	0·40	0·30	0·61	0·53
Sep	0·38	0·44	0·50	0·45	0·39	0·40	0·48	0·39	0·45	0·48
Oct	0·35	0·66	0·54	0·43	0·34	0·38	0·32	0·19	0·47	0·67
Nov	0·27	0·35	0·36	0·32	0·21	0·36	0·39	0·28	0·55	0·73
Dec	0·16	0·34	0·31	0·20	0·15	0·31	0·05	0·05	0·38	0·49

were also examined to determine the magnitude of variation to be expected in short-range transmission loss. The data in Table 47 are expressed in dB per kilometre for easy comparison. There appears to be very little difference at these ranges, for example, the total variation attributable to transmission loss between the ship and the target at 20 m depth and 250 m range is only over a 4·3 dB range for 38 observations. By 300 m range the variation has reached 7·8 dB. As target strength for schools in this region appears to vary by approximately 30 dB (Smith, unpublished data; Holliday, MS), the variation in this example does not seem to be large.

DISCUSSION

It appears from the above results that the most important effect of internal waves on fish school mapping with sonar is the variation of detection range. In one 3-day period at one 2·4 nautical mile grid, the effective range varied fivefold (Fig. 205). The magnitude of the sound velocity changes in this relatively short interval is comparable to the full range of changes in this month in this area for a 20 year climatic record. Since the precision of estimates of the effective sonar range may control the precision of estimate of the number of targets per unit area, it is imperative that an unbiased and current estimate of effective range be sought.

It would appear from these sample profiles that the estimate of target strength is not as susceptible to short-term changes as is range. As the targets are detected, measured and passed at 11–12 knots and as the usual target is less than 50 m wide (Smith, 1970), the variation in half-minute period would appear to be a relatively minor problem.

The brief field study reported above was an attempt to gain a direct measurement of internal waves at the tidal period. The results indicate that internal waves of shorter period are important sources of variation. The expense of "real-time" collection and analysis of

Table 49. An allocation of sound velocity profiles among regions and months to equalize the standard error of the maximum sound velocity gradient in the upper 30 m

Month/Region	CCI	CCO	SCI	SCO	SCS	BCI	C BCO	BCS	SBI	SBO	Total
Jan	2	2	2	2	2	2	2	2	3	2	21
Feb	2	2	2	2	2	2	2	2	2	2	20
Mar	2	2	2	2	2	2	2	2	2	2	20
Apr	8	2	6	2	2	4	2	2	5	2	35
May	3	2	10	3	3	6	2	2	6	2	39
Jun	5	6	18	6	3	10	2	2	8	8	68
Jul	17	8	25	10	6	14	6	2	36	15	139
Aug	7	17	27	14	6	15	13	7	29	22	157
Sep	11	15	20	16	12	13	18	12	16	18	151
Oct	10	35	23	14	10	11	8	3	17	36	167
Nov	6	10	10	8	3	10	12	6	24	42	131
Dec	2	10	8	3	2	8	2	2	11	19	67
Total	75	111	153	82	53	97	71	44	159	170	1015

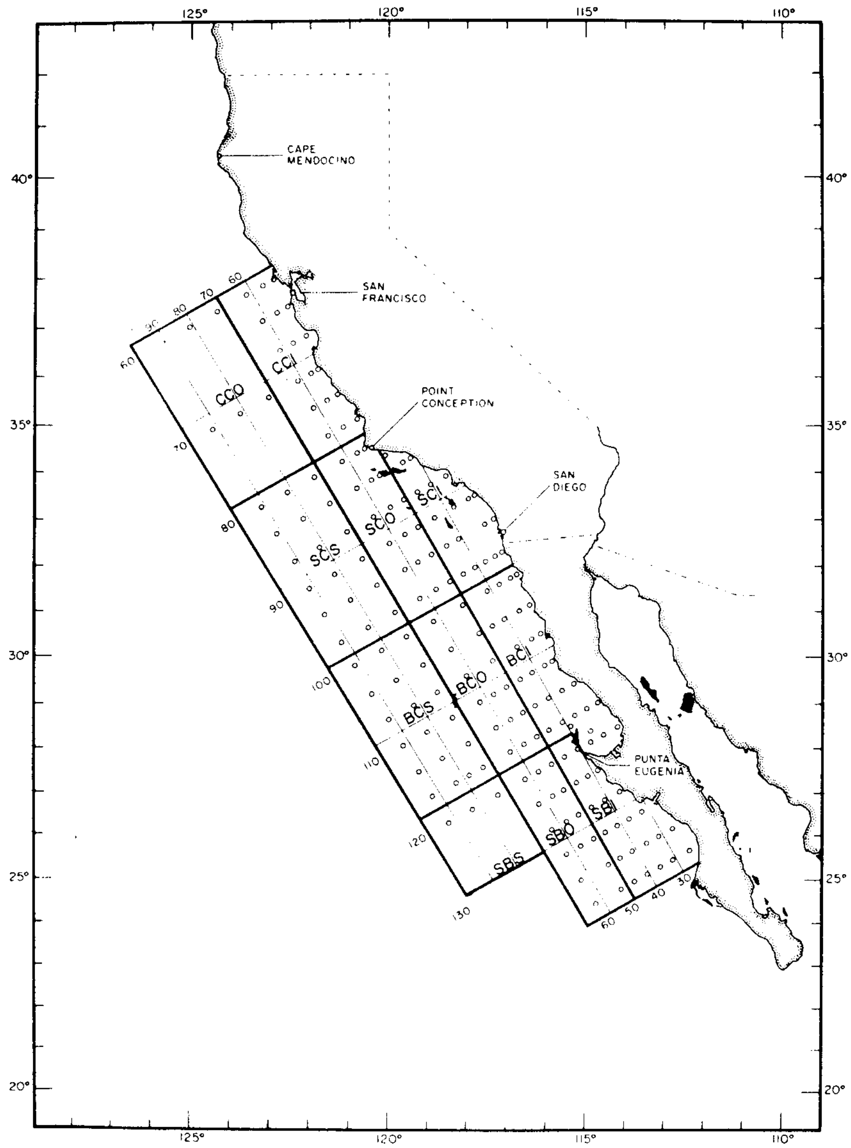

Figure 206. Regional boundaries for allocation of real-time sound velocity profiling effort. Code letters are: CC = Central California, SC = Southern California, BC = Baja California, SB = South Baja, I = Inshore, O = Offshore, and S = Seaward. The South Baja Seaward region was inadequately sampled to provide monthly profiling needs.

coherent sound velocity profiles and estimation of their resultant transmission loss appears to be prohibitive: a statistical approach is necessary.

EFFICIENT CHARACTERIZATION AND EVALUATION OF SONAR TRANSECTS

The aim here is to devise a method for the most effective overall reduction in variability in the description of effective sonar range, in space and time, using climatic data. The following steps need to be taken for a first approximation:

1) assemble historical thermal or sound velocity data by region and season;
2) partition regions and seasons by intensity of variation;

Table 50. Sonar limiting ray table

Time	Target depth (m)	Near limit (m)	Far limit (m)	Time	Target depth (m)	Near limit (m)	Far limit (m)
0351........	4	9	55	0817........	4	9	146
	10	18	238		10	18	411
	20	37	375		20	37	494
	50	82	585		50	82	677
1650........	4	9	64	1321........	4	9	73
	10	18	293		10	18	366
	20	37	430		20	37	686
	50	82	622		50	82	786

3) allocate the real-time sound velocity profiling activity among regions and seasons to reduce the standard error of the mean sound velocity gradient in the upper 30 m to a uniform value for all regions and seasons; and
4) from these real-time measurements of sound velocity, create a probability diagram to apply corrections to the numbers of targets received at various ranges and depths.

An example of this approach may be seen by reference to Tables 48 and 49. In Table 48 the long-term maximum standard deviation of the sound velocity gradient in the upper 30 m is arranged by month and region. The regions (illustrated in Fig. 206) are denoted by code letters, the first two letters of which refer to the name of a coastal section (CC = Central California; SC = Southern California; BC = Baja California; SB = South Baja) and the last letter refers to dis-

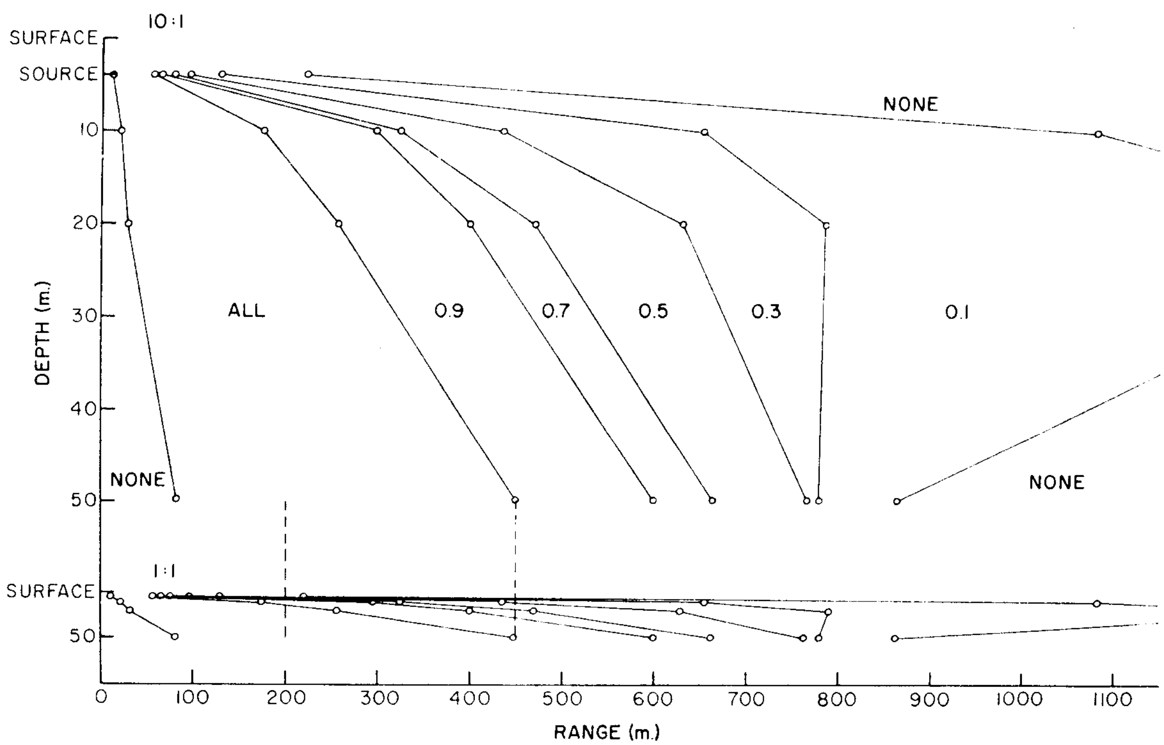

Figure 207. A pooled summary of 38 range trace analyses of limiting range by depth, contoured by the probability of detection of − 30 dB targets.

tance from the coast (I = Inshore, 0–80 miles; O = Offshore, 80–160 miles; S = Seaward, 160–280 miles). The table values are of the maximum standard deviations in sound velocity gradients expressed as m_x sec^{-1} m_z^{-1} in 5-metre intervals in the upper 30 m. The standard error of a group mean is obtained by dividing the standard deviation by the square root of the number within the group. Conversely, one may specify the number of profiles necessary to reduce the standard error of the group mean to a pre-set level by solving for N:

$$N_{ij} = \left(\frac{S_{ij}}{\text{s.e.}}\right)^2$$

where N_{ij} is the number of observations in the ith region in the jth month, S_{ij} is the maximum standard deviation of sound velocity gradient in the month/region stratum in the upper 30 m, and s.e. is the predetermined level of the standard error (ca. 0·1 m_x sec$^{-1}m_z^{-1}$ for this example.

For the purpose of this example, it was assumed that no fewer than two thermal profiles per month/region stratum would be taken. Roughly 1000 thermal or sound velocity profiles were allocated to an entire year for this example. The number of sound velocity profiles specified is reported by month and region in Table 49. It is interesting to note that the climatically derived number of profiles required for the Southern California Inshore region (SCI) in October is 23. This number of profiles would have reduced the standard error of the 10–15 m sound velocity gradient to 0·1 m_x sec^{-1} m_z^{-1} (see Table 46).

PROBABILITY DIAGRAM

The technique for pooling the sound velocity profiles in order to obtain an unbiased estimate of the water insonified by range and depth along a sonar transect, involves use of a probability diagram. The first step is to define the limiting rays for each sound velocity profile near to and remote from the ship for each target depth, given the parameters of the sonar equation. The ranges are next ordered for each target depth and probability levels are interpolated for each target depth. The array of probabilities is then contoured.

To illustrate the technique, four limiting ray calculations at four target depths have been chosen at random from the set of 38 reported above (Table 50). The limiting rays at each target depth are then ordered and interpolated ranges are calculated for probabilities of 0·75, 0·50 and 0·25 for example, and the resulting chart would be contoured at these values. An example of results for all 38 ray trace analyses is provided in Figure 207. The upper diagram is exaggerated vertically to show detail and the lower diagram is drawn on a 1:1 basis.

CONCLUSION

With respect to internal waves and the allocation of sound velocity profiling effort, two directions of research are recommended. One is to explore the optimum depth of placement of the sonar transducer with respect to internal waves and the sound velocity profile so as to minimize the shadow zones and their variation with time. The other is to explore the further allocation of sound velocity profiling effort according to the incidence of fish schools by region and by month.

ACKNOWLEDGEMENTS

The interdisciplinary nature of this research has required the counsel and direct assistance of many people over the past years. Among these have been the Captain and men of the RV "David Starr Jordan"; Drs W. H. Lenarz and C. O'Connell, J. Zweifel, T. Saur, and other colleagues at the Southwest Fisheries Center; Professors J. D. Isaacs, F. N. Spiess, V. C. Anderson, and Ms. M. Robinson of the University of California, Scripps Institution of Oceanography at San Diego: Captain P. M. Wolff, Captain S. Houston, Lt. Cdr. J. Bridenstein, T. Laevastu, Drs G. LaFond and E. Barham, and I. E. Davies and W. Batzler of the U.S. Navy; Dr T. Austin and H. Odum of the NOAA Environmental Data Service; J. Johnson of the NMFS Pacific Environmental Group; the research and training staff of Simrad in Horten, Norway, and F. Devold, L. Midttun, and O. Nakken of the Inst. Mar. Res. Bergen. The responsibility for errors and faults in interpretation of these data lie solely with the author. Technical and numerical assistance was received from Nancy Wiley, R. C. Counts, Esther Barker, and J. Thrailkill.

REFERENCES

Couper, B. K. & La Fond, E. C. 1970. The mechanical bathythermograph, an historical review. Advances in instrumentation, Instrument Soc. Amer., 25(3): 735–70.

Smith, P. E. 1970. The horizontal dimensions and abundance of fish schools in the upper mixed layer as measured by sonar. *In* Proc. int. Symp. on Biological Sound Scattering in the Ocean. Ed. G. Brooke Farquhar. Oceanography of the Navy Maury Center Rep. (005).